

## SUPPORTING INFORMATION

### Supplementary methods

#### DNA extraction and genotyping

Isolation of genomic DNA from peripheral blood leukocytes or from whole blood samples was performed using the FlexiGene DNA Kit (Qiagen, Hilden, Germany) according to the manufacturer's instruction. An overview of the analysed SNPs is given in supplementary table 2. Genotyping was done by PCR and melting curve analysis in a LightCycler® 480 instrument (Roche Diagnostics, Mannheim, Germany) using fluorescence resonance energy transfer (FRET) probes (TIB MOLBIOL, Berlin, Germany). PCR was performed in a total volume of 5 µl containing 10-50 ng genomic DNA, Light Cycler 480 Genotyping Master reagent (Roche Diagnostics), 2.5 pmol of each primer and 0.75 pmol of each FRET probe. Amplification was set with an initial denaturation step of 95°C for 10 min followed by 45 cycles of 95°C for 10 s, primer annealing temperatures for 10 s (see supplementary table 3) and 72°C for 15 s. For melting curve analysis, an initial denaturation step of 95°C for 1 min was followed by rapid lowering of the temperature to 40°C for 30 s and continued with a slow temperature increase up to 80°C. Fluorescence intensity was measured continuously (1 acquisition/°C). Sequences of primers and FRET probes as well as the primer annealing temperatures used for typing SNPs in the RLH pathway are shown in supplementary table 3. For typing of rs12979860 in the IL-28B gene the corresponding LightMix Kit from TIB MOLBIOL (Berlin, Germany) was used according to the manufacturer's instructions.

#### Statistical analyses of the genetic data

Each genetic marker was tested for Hardy-Weinberg equilibrium in the control population and, with exception of rs10813831 in RIG-I, was found to be in Hardy-Weinberg equilibrium. rs1990760 is in Hardy-Weinberg equilibrium if the SRH and CH groups are analysed together, but is not in each group separately. rs3747517 is in Hardy-Weinberg equilibrium in the CH group but not in the SRH group. For comparison between categorical variables, Fisher's exact test or Chi square test was used where appropriate.

In order to avoid type I errors due to multiple comparisons, we replicated the result for rs3747517 in a second independent cohort instead of using Bonferroni-type corrections.

Data were evaluated using the SPSS 16.0 software (SPSS Inc.-IBM, Armonk, NY).

Haploview software was used to generate linkage disequilibrium plots for the analysed genes.

The allele frequencies of SNPs tested in our study cohorts fit to the frequencies published for the CEU reference population by the HapMap project (as accessed from HapMap project data release 27).

### **Plasmids and site-directed mutagenesis**

The MDA-5 variants encoded by the analyzed SNPs were generated using an HA-tagged MDA-5 construct in the pSfiExpress vector and site-directed mutagenesis. Primer sequences for site-directed mutagenesis are given in supplementary table 6. For HCV replication assays, the MDA-5 variants were subcloned into SCRPSY-DEST lentiviral vector (kindly provided by Paul Bieniasz, The Rockefeller University), co-expressing RFP and puromycin resistance.

### **Generation of ISG-expressing lentiviral particles**

Lentiviral pseudoparticles were generated by co-transfecting  $5 \times 10^5$  293T cells in T25 flasks with plasmids expressing the pSCRPSY proviral DNA, HIV-1 gag-pol and VSV-G in a ratio of 25/5/1, respectively. For each transfection, 60  $\mu$ l XtremeGene9 (Roche Diagnostics, Mannheim, Germany) was combined with 20  $\mu$ g total DNA in 140  $\mu$ l Opti-MEM (Gibco, Life Technologies, Carlsbad, CA). Transfections were carried out for 12 h, followed by a medium change to DMEM containing 1.5% FBS. Supernatants were collected at 72 h, cleared by centrifugation and filtered through a 0.45  $\mu$ m pore size syringe filter. Before freezing, samples were adjusted to final concentrations of 20mM HEPES and 4  $\mu$ g/ml polybrene were added, and aliquots stored at  $-80$  °C.

### **Determination of gene expression by rt-PCR**

At the indicated time points total cellular RNA of HEK 293 or Huh-7.5 cells was isolated using peqGold Total RNAKit (peqlab, Erlangen, DE) according to the manufacturer's protocol. RNA was reverse-transcribed using oligo-dT primers and mRNA levels were analysed by RT-PCR using gene-specific primers and probes from the Roche universal probe library (Roche Diagnostics, Mannheim, Germany). The following primer and probe combinations were used: IP-10 (primer 1: gaaagcagtttagcaaggaaaggt; primer 2: gacatatactccatgtagggaagtga; probe #34); IFN- $\beta$  (primer 1: cgacactgttcgtgtgtca; primer 2: gaggcacaacaggagagcaa; probe #25); ISG15 (primer 1: gcgaactcatcttgccagt; primer 2: ttcagctctgacaccgacat; probe #76); IL-28B (primer 1: agggccaaagatgcctta; primer 2: cagctcagcctccaaagc; probe #60); ISG56 (primer 1: agaacggctgcctaatttacag; primer 2: gctccagactatccttgacctg; probe #9); neomycin phosphotransferase gene (*npt*) (primer 1:

ggcaggatctcctgtcatct; primer 2: catcagccatgatggatacttct; probe#51); HPRT (primer1: tgaccttgattattttgcataacc; primer 2: cgagcaagacgttcagtct; probe#73)

The relative abundance of target transcripts was normalized to the expression levels of HPRT in experiments with Huh-7.5 cells and to the npt gene in overexpression experiments in HEK293 cells to equalize potential differences in transfection efficiencies.

### **Western blot analyses**

For each functional assay protein expression levels were examined by western blot. Rabbit polyclonal antibodies against MDA-5 were purchased from Abcam (ab69983; Cambridge, UK), mouse antibodies against RFP from Cell Biolabs (AKR-021; San Diego, CA), antibodies against the HA-tag were from Santa Cruz (sc-805; Dallas, Texas) and HRP-coupled beta-actin antibody from Sigma (A3854; Deisenhofen, Germany). Band intensities were measured using ImageJ 1.45s software.

## Supplementary tables

**Supplementary table 1.1:** Cohort 1

	<b>Patients with spontaneously resolved hepatitis C</b>	<b>Patients with chronic hepatitis C</b>
Number	76	199
Gender	m: 35 (46.1 %) f: 41 (53.9 %)	m: 84 (42.2 %) f: 115 (57.8 %)
Origin	Germany: 44 (57.9 %) Ireland: 28 (36.8 %) Southern Europe: 2 (2.6 %) Eastern Europe: 2 (2.6 %)	Germany: 123 (61.8 %) Ireland: 48 (24.1 %) Eastern Europe: 16 (8.0 %) Russia: 10 (5.0 %) Southern Europe: 2 (1.0 %)

**Supplementary table 1.2:** Cohort 2

	<b>Patients with spontaneously resolved hepatitis C</b>	<b>Patients with chronic hepatitis C</b>
Number	209	310
Gender	m: 75 (35.9 %) f: 134 (64.1 %)	m: 161 (51.9 %) f: 149 (48.1 %)
Origin	Germany: 209 (100 %)	Germany: 310 (100 %)

**Supplementary table 2:** Characterization of genotyped polymorphisms in DDX58, IFIH1, MAVS, DHX58 (rs number, chromosomal position, alleles, position in gene and AA substitution)

<b>Genotyped polymorphisms in the DDX58 gene (RIG-I), Chr. 9</b>				
ID	Chromosomal position	Alleles	Position in gene	AA substitution
rs10813831	32526146 (accession no.: NT_008413.18)	C/T	Exon 1	Arg/Cys
rs11795404	32492412 (accession no.: NT_008413.18)	C/A	Exon 4	Ser/Ile
rs35527044	32489363 (accession no.: NT_008413.18)	T/G	Exon 6	Thr/Pro
rs951618	32487627 (accession no.: NT_008413.18)	A/G	Exon 9	Ile/Thr
rs17217280	32480251 (accession no.: NT_008413.18)	T/A	Exon 12	Asp/Glu
rs35253851	32459483 (accession no.: NT_008413.18)	G/T	Exon 17	Phe/Leu
<b>Genotyped polymorphisms in the IFIH1 gene (MDA-5), Chr. 2</b>				
ID	Chromosomal position	Allele	Position in gene	AA substitution
rs10930046	163137983 (accession no.: NT_005403.17)	A/G	Exon 7	His/Arg
rs3747517	163128824 (accession no.: NT_005403.17)	C/T	Exon 13	Arg/His
rs35667974	163124637 (accession no.: NT_005403.17)	A/G	Exon 14	Ile/Val
rs1990760	163124051 (accession no.: NT_005403.17)	T/C	Exon 15	Thr/Ala

---

**Genotyped polymorphisms in the VISA gene (MAVS), Chr. 20**


---

ID	Chromosomal position	Allele	Position in gene	AA substitution
rs7262903	3843027 (accession no.: NT_011387.8)	C/A	Exon 5	Gln/Lys
rs7269320	3846397 (accession no.: NT_011387.8)	C/T	Exon 7	Ser/Phe

---



---

**Genotyped polymorphisms in the DHX58 gene (Lgp2), Chr. 17**


---

ID	Chromosomal position	Allele	Position in gene	AA substitution
rs2074158	40257163 (accession no.: NT_010783.15)	A/G	Exon 10	Gln/Arg
rs2074160	40255812 (accession no.: NT_010783.15)	G/A	Exon 12	Arg/Gln

---

**Supplementary table 3:** Primer sequences, FRET probe sequences, and primer annealing temperatures used for genotyping variants in the genes DDX58, IFIH1, VISA and DHX58.

Polymorphism	Primer sequences	Primer annealing	FRET probe sequences
rs10813831	CCATGTAGCTCAGGATGTAGGT AACGTAGCTAGCTGCAAGCAGA	60°C	TGCAGGCTGCATCGCTGC-FL LC670-CGGTGGTCATGCCGGCCTCTG
rs17217280	CCTCTGAAAACACCACTCACCTT ACGAATGAAAGATGCTCTGGATTACT	60°C	GCTCAATCTCATCGAATCCTGC-FL LC670-GCTCGGACATTGCTGAAGAAGTCTTTC
rs11795404	ATGAGCGAGTCCTAAGTAGAG GAATGCCTTCTCAGATCAGA	60°C	CCACAGTTCACTGAACTTGTTCC-FL LC670-CTTTCTCCAAAGCAAGTTTCAAAGTTTTGG
rs35527044	CAGAAAACTATGTAAGTAATGGC CAGAATTTGTGGACATTAGACT	60°C	GCACATATTATTGTGTTTTTTCCTTTC-FL LC670-TAGCAGGCAAAGCAAGCTCTAATTGGT
rs951618	ACTGACGCATCAAGAGAAGCAC TTGTGGAAACATTGTACCATTTCTCA	60°C	TCCTTACAGGTCACTGGGCT-FL LC670-ACTGCCTCGGTTGGTGTGGG
rs35253851	GCAGAGCAGTTTTTTATTTTCCTTA CGTATCTGTGCCTGTTTCTTGCTA	60°C	CAGACTCATGAAAAATTCATCAGAGA-FL LC670-AGTCAAGAAAAACCAAACCTGTACCTG
rs1990760	CCCACAGCAATTTACTCACCTG GAGCTCCAGGTCCAATAACCC	60°C	AGAAAACAAAACACTGCAAAGA-FL LC670-GTGTGCCGACTATCAAATAAATGGTGA
rs3747517	ACAATACCTTATGAGCATACTCCTC CAGAGCTGATGAGAGCACC	55°C	AACTGTCTCACGTTTCGATAACTCC-FL LC670-GAACCACTGTGAGCAACCAGGACGT
rs10930046	AGTCCCAGTATCTGAGGAAGG TGCTGATATGGAGAAATGAACTCT	60°C	TGCATCAAATAACGCCTCATG-FL LC670-TGTTATTATACTGCTTCTTTGTTGGTGTGA
rs35667974	GAAAACCAAGAGAAATATTGCCA GAGGCTAAAGGAGAGGAAGTTG	60°C	AAGATATCCATGTAATTGAGAAAATGCA-FL LC670-CACGTCAATATGACCCCAAGATTCAAGT

rs7262903	AGCAAGCCCTGCAGACG CCAGATGGGGCAACTCTA	60°C	CAGTTCTGTGTCCTT <u>CT</u> CCTGA-FL LC670-CCCGCTGGAGGTCAGAGGGCT
rs7269320	GGCAGCTCAGCCTGGCTA CTGATGGCAAGATCCTCGAA	60°C	AGGCTTACTCAGCTCCGACCCAAG-FL LC670-CCCCTATTCTCAA <u>A</u> AGCTGCTGTC
rs2074158	GTCAAGAGCCCATAACGCAC TACCAGCCTCTTTCTCCTCCC	60°C	GCAAGAAGTGATCC <u>A</u> GAAGTTCCAAG-FL LC670-TGGAACCCTGAACCTTCTGGTGGCC
rs2074160	TTCCACAGGTCTCACGAG CTTCCAGGTACAAATGATCTTAGT	60°C	CCACCCCAGATCC <u>A</u> GGATCT-FL LC670-CAGCAGGCAGCCTTGACCAAG

FL: Fluorescein, LC670: LightCycler-Red 670. The polymorphic position within the sensor probe is underlined. A phosphate is linked to the 3'-end of the anchor probe to prevent elongation by the DNA polymerase in the PCR.



**Supplementary table 4:** Genotype frequencies of MDA-5: A946T (rs1990760), cohort 1, 2 and combined analysis

Analysed group	CH	SRH	CH	SRH	CH	SRH
	Cohort 1		Cohort 2		Combined analysis	
Genotype	Frequency (%)		Frequency (%)		Frequency (%)	
TT	73 (37.4%)	22 (28.9%)	108 (35.0%)	84 (44.0%)	181 (35.9%)	106 (39.7%)
CT	96 (49.2%)	40 (52.6%)	142 (46.0%)	71 (37.2%)	238 (47.2%)	111 (41.6%)
CC	26 (13.3%)	14 (18.4%)	59 (19.1%)	36 (18.8%)	85 (16.9%)	50 (18.7%)
p-value	<b>0.33</b>		<b>0.09</b>		<b>0.40</b>	

p-value by  $\chi^2$  test for genotype distribution. CH, chronic hepatitis. SRH, spontaneously resolved hepatitis.

**Supplementary table 5.1:** MDA-5 haplotype frequencies composed of R843H (rs3747517; T = minor allele/ C = major allele) and T946A (rs1990760 ; C = minor allele/ T = major allele)

Haplotype (R843H/T946A)	CH	SRH	Control
Minor allele/minor allele H843/A946	113 (16.4%)	65 (18.8%)	89 (12.2%)
Minor allele/major allele H843/T946	2 (0.3%)	23 (6.6%)	42 (5.8%)
Major allele/minor allele R843/A946	135 (19.6 %)	51 (14.7%)	167 (22.9%)
Major allele/major allele R843/T946	438 (63.7%)	207 (59.8%)	430 (59.1%)

CH, chronic hepatitis. SRH, spontaneously resolved hepatitis.

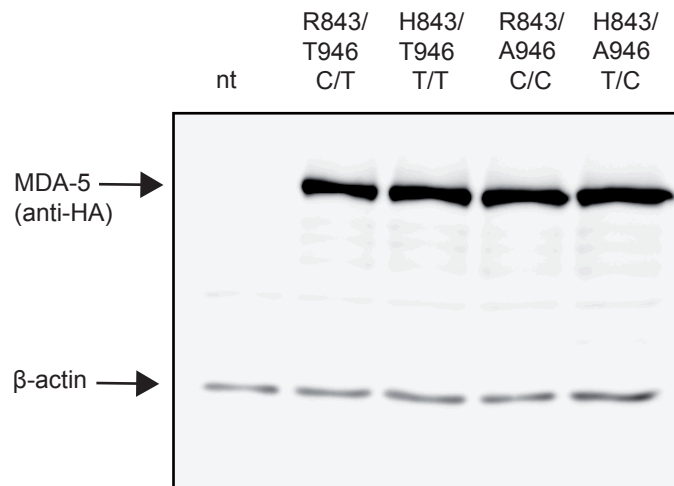
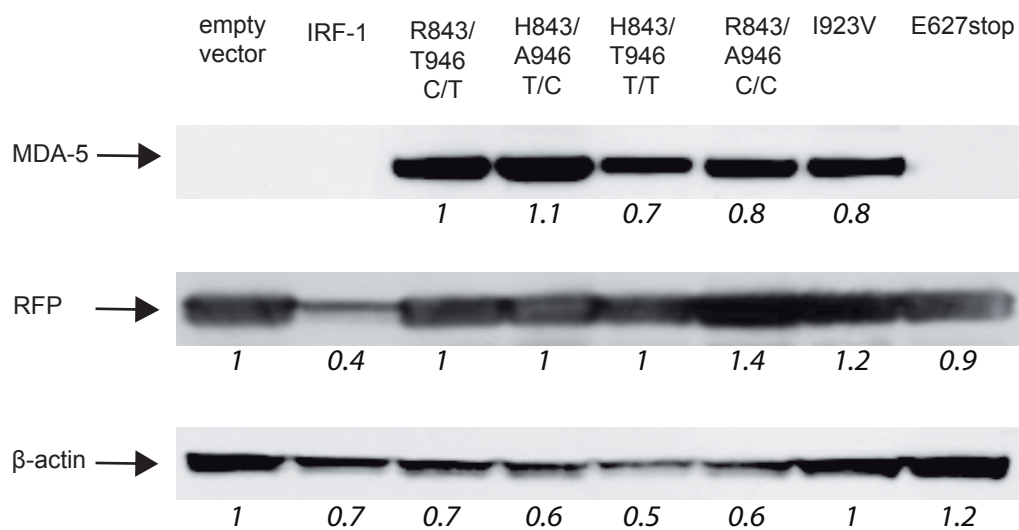
**Supplementary table 5.2:** Allele, genotype and carrier frequencies of haplotype T = minor allele at rs3747517 (R843H) and T = major allele at rs1990760 (T946A) in MDA-5; combined cohorts

Haplotype T/T (R843H/ T946A)	Control	CH	SRH	p-value	OR (95% CI)
	Frequency (%)				
+	42 (5.8 %)	2 (0.29 %)	23 (6.6 %)	<b>3.4 x 10<sup>-10</sup></b>	<b>24.42</b> <b>(5.72 – 104.26)</b>
-	686 (94.2 %)	686 (99.7 %)	323 (93.35 %)		
++	8 (2.2 %)	0 (0 %)	8 (4.6 %)	<b>4.5 x 10<sup>-6</sup></b>	
+-	26 (7.1 %)	2 (0.6 %)	7 (4.0 %)		
--	330 (90.7 %)	342 (99.4 %)	158 (91.3 %)		
++ or +- --	34 (9.3 %) 330 (90.7 %)	2 (0.6 %) 342 (99.4 %)	15 (8.7 %) 158 (91.3 %)	<b>1.1 x 10<sup>-6</sup></b>	<b>16.23</b> <b>(3.67 – 71.87)</b>
++ --	8 (2.2 %) 330 (90.7 %)	0 (0 %) 342 (99.4 %)	8 (4,6 %) 158 (91.3 %)	<b>4.4 x 10<sup>-5</sup></b>	<b>36.74</b> <b>(2.11 – 640.86)</b>

p-value by Fisher's exact test or  $\chi^2$  test for haplotype distribution comparing CH versus SRH. CH, chronic hepatitis. SRH, spontaneously resolved hepatitis. OR, odds ratio. CI, confidence interval. "+" haplotype present; "-" haplotype absent.

**Supplementary table 6:** Primer sequences used for site-directed mutagenesis of MDA-5

<b>Amino acid change</b>	<b>Protein</b>	<b>Primer sequences (5' → 3')</b>
H843R (histidine substituted for arginine at position 843)	MDA-5	CACAGTGGTTCAGGAGTTATCGAACGTGAGACAGTTAATGATTTCCG CGGAAATCATTA ACTGTCTCACGTTTCGATAACTCCTGAACCACTGTG
A946T (alanine substituted for threonine at position 946)	MDA-5	CTTTACATTGTAAGAGAAAACAAAACACTGCAAAAGAAGTGTGCCGAC GTCGGCACACTTCTTTTGCAGTGTTTTGTTTTCTCTTACAATGTAAAG
I923V (isoleucine substituted for valine at position 923)	MDA-5	CTGGGGAAGATATCCATGTAGTTGAGAAAATGCATCACGTC GACGTGATGCATTTTCTCAACTACATGGATATCTTCCCCAG
E627stop (a stop codon substituted for glutamic acid at position 627)	MDA-5	GATAGATGCGTATACTCATCTTTAACTTTCTATAATGAAGAG CTCTTCATTATAGAAAGTTTAAAGATGAGTATACGCATCTATC

**A****B**

### Supplementary figure 1: Expression level of MDA-5 variants in HEK 293 cells and HU7.5 cells

**A:** HEK 293 cells were transfected with plasmids coding for the indicated HA-tagged MDA-5 variants defined by the four possible amino acid combinations at the amino acid positions 843 and 946 coded by the SNP alleles T/C at rs3747517 and T/C at rs1990760 respectively. 24 hours after transfection cells were harvested and the expression of the MDA-5 variants was analysed by western blot using anti-MDA-5 antibodies.

One representative experiment of several performed using different batches of plasmid preparation is shown.

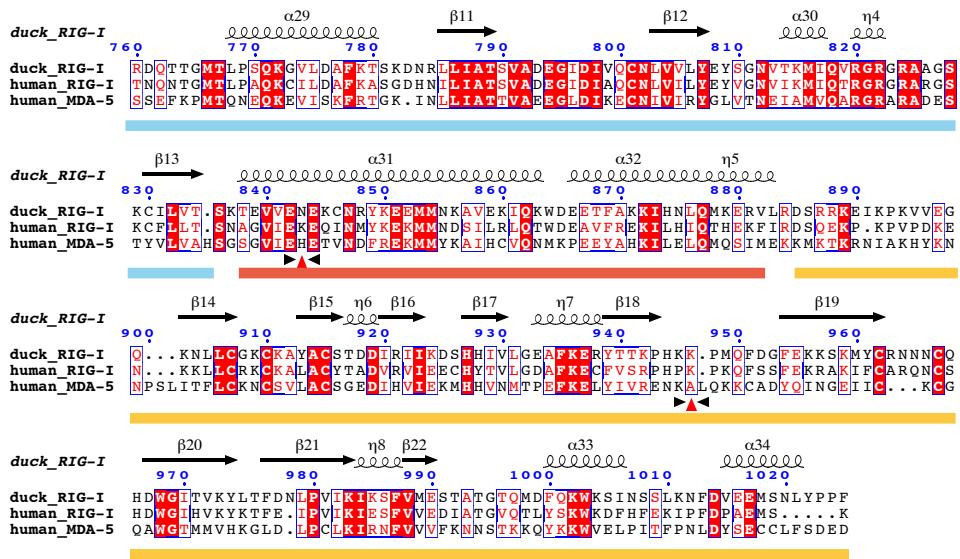
**B:** Huh-7.5 cells were transduced with lentiviral vectors expressing RFP and the indicated MDA-5 variants.

An empty vector and a construct coding for IRF-1 served as controls. 72 hours after transduction cells were harvested and protein expression was analysed by western blot using antibodies against MDA-5, RFP and  $\beta$ -actin. Relative intensities as determined by Image J are depicted below the bands.

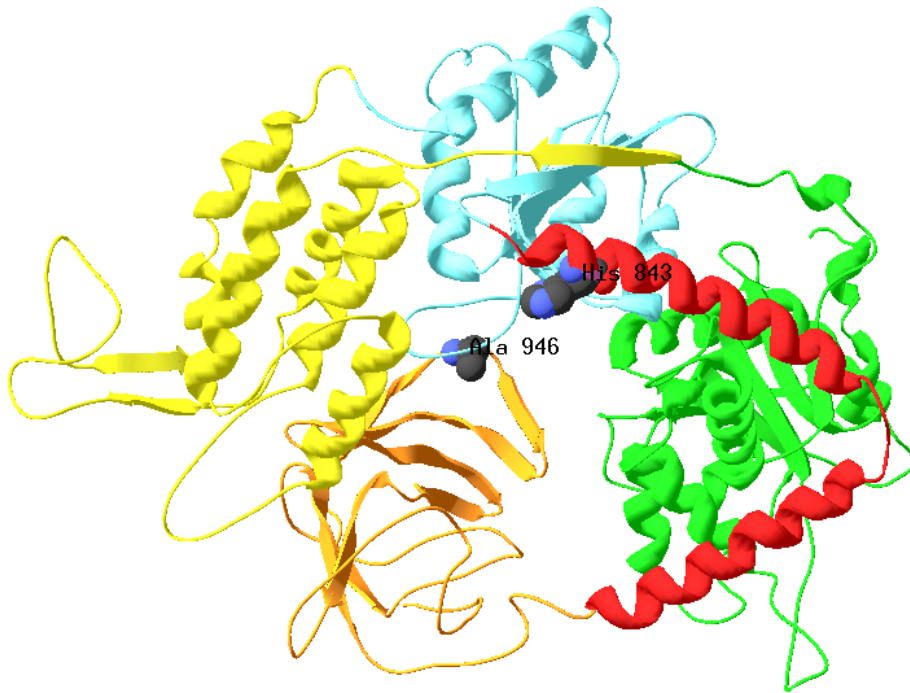
The expression patterns varied slightly between experiments without consistent differences between the variants.

No correlation of variation in expression level and activity in the simultaneously performed functional assays was seen.

A



B



Supplementary figure 2

## **Supplementary figure 2: Position of AA 843 and AA 946 in a structural model of MDA-5**

MDA-5 and RIG-I have high sequence homology and share the same domain architecture consisting of two N-terminal tandem caspase activation and recruitment domains (CARDs), a central DECH-box RNA helicase, and a C-terminal domain (CTD). The DECH-box RNA helicase in RIG-I and MDA-5 comprises the helicase 1 domain (green), the helicase 2 insertion domain (yellow), the helicase 2 domain (cyan) and the pincer domain (red) connecting it to the CTD (orange)

### **A: Sequence alignment of AA 760 – AA 1025 of human MDA-5 to duck RIG-I and human RIG-I.**

Amino acids are numbered according to their position in human MDA-5. Superposed above the sequences is the secondary structure derived from duck RIG-I according to Kowalinski et al. (Cell 147, 423-35, 2011). The structural domains are indicated by bars below the sequence (color code given above). Positions identical in all sequences are white against a red background. Positions with high similarity are red against a white background. Red triangles below the alignment indicate the position of the amino acids 843 and 946 encoded by the T/T haplotype. Alignment was prepared with Clustalw and ESPript (<http://esprict.ibcp.fr/ESPript/cgi-bin/ESPript.cgi>).

### **B. Structural model of MDA-5 without the N-terminal CARD domains.**

The domains are color-coded as indicated above. The model was generated using SWISSMODEL and is based on the human RIG-I structure 3tmiA integrating solved structures for the MDA-5 CTD (2rqb and 3ga3) and MDA-5 helicase 1 domain (3b6e). As indicated AA 843 locates within the elbow-like pincer motif (AA 843 of MDA-5 is equivalent to position 751 in the  $\alpha$ -helix 31 of RIG-I). AA 946 in MDA-5 locates within the loop 944 – 949 in the CTD (the loop 944 – 949 in MDA-5 is equivalent to the loop 849-857 in RIG-I).

The pincer structure is proposed to open and close upon RNA binding thereby altering the orientation of the CTD to the helicase domains. This transmits the signal (RNA and ATP binding) to the CARDs by releasing them from their auto-repressed state. Furthermore AA843 is directly adjacent to AA 841/2 described to be part of the head surfaces of the putative contact interface between MDA5 monomers in the filamentous MDA-5 multimers that form along dsRNA (Wu et al. Cell,152:276-289). Mutating the neighboring AA (I842 and E841 to R) of H843 reduced the formation of MDA-5-filaments and strongly reduced signaling strength induced by poly I:C. The loop 849-857 in RIG-I strongly changes conformation upon dsRNA binding allowing the central Phe855 to stack on the end of the first RNA base pair of the RIG-I ligand (Kowalinski et al. and Luo et al. Cell 147, 409-35 (2011)). In the recently published structure of MDA-5 bound to a dsRNA ligand the position of the CTD-loop could not be determined in the 3D structure. This is interpreted by the authors that the loop might be mobile during ligand binding and has to move out of the way to allow the binding of the dsRNA backbone. Deletion of the CTD-loop inhibited signaling strength (Wu et al. Cell,152:276-289).

SNPs changing AA at 843 and 946 are therefore plausible to influence the activity of MDA-5 in view of their central position in structural domains of MDA-5 required a) to adjust the fitting of RLHs to their ligands and b) to transform RLHs into their signaling competent state by liberating the card-signaling domains and by the induction of head to tail MDA-5 multimer-formation out of MDA-5 monomers along the dsRNA ligand (Wu et al. Cell,152:276-289 (2013)). The complementary function of the pincer domain and the loop in the CTD fitting the RNA-ligand seem compatible with synergism between these two specific amino acids as seen in our study.